JAERI-M
6874

NONSTOICHIOMETRY IN URANIUM SESQUINITRIDE

December 1976

Hiroaki TAGAWA

日本原子力研究所
Japan Atomic Energy Research Institute

JAERI-M 6874

Nonstoichiometry in Uranium Sesquinitride

Hiroaki TAGAWA

Division of Chemistry, JAERI

(Received December 17, 1976)

Of four phases in the U - N system, the sesquinitride with an Mn_2O_3-type body-centered cubic structure, α-U_2N_3, exhibits a wide nonstoichiometric range of composition. The defect characteristic of α-U_2N_3 has been examined from the standpoint of crystal structure and thermodynamic properties. From the variation of the lattice parameter in the U_2N_3 - UN_2 system, two separated linear relationships between lattice parameter and the N/U atom ratio are obtained: one is characteristic of U_2N_3 and the other of UN_2. Using the density data, it is deduced that the nonstoichiometry in U_2N_3 is caused by the interstitial nitrogen atoms, and the nonstoichiometry in UN_2 is due to the nitrogen vacancies. X-ray and neutron diffraction analyses also show that the excess nitrogen atoms fill the vacant interstitial positions without any structure change. Thermodynamic data suggest that the excess nitrogen is simply dissolved in U_2N_3 with the wide homogegeous range of composition; the results are consistent with those obtained from the measurements for lattice parameter and density, and from the structure analysis.

JAERI-M 6874

三窒化二ウランの非化学量論性

日本原子力研究所東海研究所
原子炉化学部

田川　博章

（1976年12月17月受理）

ウラン－窒素系の4相の中で，Mn_2O_3型体心立方構造を持つ三窒化二ウランα－U_2N_3は広い非化学量論組成幅を有する。そこで結晶構造と熱力学性質の立場からα－U_2N_3の欠陥構造の性質を調べた。U_2N_3－UN_y系の格子定数の変化から，格子定数とN/U原子比との間に2つの直線関係の存在することが見出された：1つはU_2N_3の特性であり，他はUN_yの特性である。密度の測定値を使うと，U_2N_3の非化学量論性は窒素の格子間割込み原子によって惹起され，UN_yの非化学量論性は格子点位置の窒素原子の欠陥によって生成することがわかる。X線と中性子回折の結果は過剰窒素が結晶構造の変化なしにU_2N_3の格子間割込み位置に入ることを示す。窒素圧の測定から求めた熱力学的性質は過剰窒素が幅の広いU_2N_3均一相に単純に溶けることを示唆する；この結果は格子定数，密度の測定結果から得られた結論，および構造解析から得られた結論と予盾しない。

目　次　な　し

1. Introduction

The use of uranium mononitride as an advanced nuclear fuel is being considered, because it possesses many essential properties such as high uranium density, high thermal conductivity, high melting temperature, large negative enthalpy of formation, etc. Interest in the mononitride, therefore, has generated many studies of the U - N system.

Of many nitrides, we feel great interest in the physical and chemical properties of uranium nitride. The reasons are as follows: there are different bonding types of the nitride — the mononitride is metallic, and the sesquinitride is rather ionic; the sesquinitride with a cubic structure is a nonstoichiometric compound, which has a wide range of composition; thus it has been considered that the cubic sesquinitride makes the continuous solid solution connected to the dinitride; and the phase relations of the U - N system are analogous to those of the Am - O and Cm - O systems in the actinide - oxygen systems. Thus the structural and thermodynamic properties of uranium nitrides, especially of the cubic sesquinitride, have been examined with emphasis on nonstoichiometry.

2. General Survey of Nitrides

Most elements form rather stable compounds by the reactions with nitrogen. They are called nitrogen compounds, and many of them are known by the name of nitride. So-called nitride is applied to those compounds in which nitrogen is combined with elements of lower or about equal electronegativity. The nitrides, which so far are known, are summerized in Table I. The following metals are not known to form nitrides or to be in a pure state: K, Rb, Cs, Au, Ru, Rh, Pd, Os, Ir and Pt. Nitrides of the transition metals generally have the formulas, Me_2N and MeN. The nitrides of Mn, Fe, Co and Ni form a group of less stable compounds of greater complexity than those of the other transition metal nitrides. The lanthanide and actinide nitrides are expressed by the formula MeN. All the nitrides except Th_3N_4, U_2N_3 and UN_2 have the composition of the Nitrogen-to-Metal ratio equal unity or less. In the table, the line above a formula shows to be the nonstoichiometric nitride.

From the nature of the chemical bonding, nitrides can be usually

classified into three types: ionic, covalent and metallic. In some cases, an element forms nitrides of quite different types: e. g. one nitride shows the behavior as an ionic compound, and another has the characteristic of a metallic conductor.

(1) Ionic nitrides are formed from Li, Na, Group IIA metals, and Zn and Cd. Their formulas, Me_3N and Me_3N_2, correspond to what result from combinations of the metal ions with the N^{3-} ions, as $Li^{+}_{3}N^{3-}$. The radius of the N^{3-} ion in these nitrides would appear to be close to 1.5 A. All the ionic nitrides are of stoichiometric composition.

(2) Covalent nitrides are formed from the elements of Groups IIIB, IVB and VB. There are various covalent nitrides, and their properties vary greatly depending on the element with which nitrogen is combined. They also are stoichiometric compounds.

(3) Metallic nitrides are formed by the transition metals, including the lanthanide and actinide elements. The metallic nitrides, so-named because of their physical similarity to refractory hard metals, are often called interstitial nitrides. In the nitrides, the metal atoms are approximately, or in some cases exactly close-packed. Compounds of the type Me_2N are generally derived from hexagonal close-packing, and those of the type MeN from cubic close-packing. These nitrides are often not exactly stoichiometric compounds, and have a tendency to result in the nitrogen-deficient. The deviation from the stoichiometric composition occurs a variation in physical and chemical properties. Therefore, unless the stoichiometry is given, observed values have no meaning whatever. As shown in the table, the heminitrides of Ti, V, Nb, Ta and Cr, the mononitrides of Ti, Zr, Hf and V, and the sesquinitride of U, have wide ranges of composition.

3. Phase Relations in the U - N System

3.1. Phase Diagram

In the U - N system, four phases are characterized: mononitride, cubic and hexagonal sesquinitrides and dinitride. The mononitride UN is

stable from room temperature to its melting point of 2830°C in 5 atm N_2. In the sesquinitride there are two modifications: Mn_2O_3-type body-centered cubic U_2N_3 and La_2O_3-type hexagonal close-packed U_2N_3. Both U_2N_3 are not allotropic modifications of the same compound, but they are conventionally designated as α- and β-U_2N_3, respectively. α-U_2N_3 exhibits a wide nonstoichiometric range of composition: i. e. $UN_{1.54}$ - $UN_{1.75}$. β-U_2N_3 is a nearly stoichiometric compound. The α → β transition occurs above 800°C[6,16,30]. The decomposition temperature of U_2N_3 at 1 atm pressure of nitrogen is 1350°C. The dinitride UN_2 occurs at the N/U atom ratio beyond 1.75, but has never been obtained as a stoichiometric compound. The phase diagram is shown in Fig. 1[31]. A few of the phase boundaries are still in doubt and these are represented by dashed lines.

3.2. The UN Phase

UN, which is of a NaCl-type face-centered cubic structure[26], has a narrow range of stoichiometry from room temperature to about 1100°C. At higher temperatures UN has a slightly tendency to broaden its range of stoichiometry and dissolves limited amounts of either uranium or nitrogen. The composition range is between 0.991 and 1.005 as N/U atom ratio[5,7, 15].

3.3. The U_2N_3 Phase

α-U_2N_3 is a hyperstoichiometric compound with an Mn_2O_3-type body-centered cubic structure[26]. The U-rich phase boundary has been determined from tensiometric measurements[10,19,23,29]. The isotherms of nitrogen pressure - composition of the UN - UN_2 system show bending at $UN_{1.54}$[10,29]. The N-rich phase boundary is taken to be at approximately $UN_{1.75}$ from the lattice parameter versus composition data of Fig. 2[30].

β-U_2N_3 had been reported to have the composition range, $UN_{1.34}$ - $UN_{1.51}$[5,6,27,28]. However, the structural analysis[22] and the observations of the phase[6,7] show that the composition of the nitride is close to the stoichiometric. The structure is a La_2O_3-type hexagonal close-packed[22,36].

3.4. The UN_2 Phase

UN_2 is assigned to have a CaF_2-type face-centered cubic structure[26]. This phase occurs above the N/U atom ratio of 1.75, but is not obtained at the N/U ratio beyond 1.80[34].

4. Defect Types of U_2N_3 and UN_2

The defect type of a nonstoichiometric compound can be known by determining lattice parameter and density of the compound as a function of composition.

4.1. Lattice Parameter Change in the U_2N_3 - UN_2 System

Figure 2 shows the variation of the lattice parameters of U_2N_3 and UN_2 determined as a function of the N/U atom ratio. It is divided into the three regions: the two-phase region of α-U_2N_3 + UN or α-U_2N_3 + β-U_2N_3, the single α-U_2N_3 phase, and the UN_2 phase. In the two-phase region, the lattice parameter of α-U_2N_3 prepared under various conditions is the constant value, 10.684 A. As nitrogen is added to the structure, the nitride results in the single phase of α-U_2N_3. The lattice parameter value decreases linearly with increase of the N/U ratio. This tendency, which is the characteristic of the ionic bond, is opposite to that in the case of MeN. The lower existence limit of the phase is taken to be $UN_{1.54}$. The composition is in good agreement with those determined by the tensiometric measurements: $UN_{1.535-1.545}$[10] and $UN_{1.542}$[29]. The upper limit is determined at $UN_{1.75}$.

For the nitride with the N/U atom ratio of 1.76, it was found that X-ray powder diffraction patterns lacked weak reflection. This indicates that the transformation of the Mn_2O_3-type b. c. c. structure into the CaF_2-type f. c. c. structure. At the same time, the lattice parameter of the CaF_2-type becomes half the value of the Mn_2O_3-type structure. In addition, the lattice parameter of $UN_{1.76}$ drops by about 0.02 A from 5.32 A, which is half the value for U_2N_3 at $UN_{1.75}$.

In order to know what the lattice parameter varies with the N/U atom ratio in the U_2N_3 - UN_2 system, the lattice parameter for the stoichiometric UN_2 should be estimated. It was obtained by using the known values for uranium nitrides and americium oxides. As given in Table II, the

ratio of the lattice parameter for an americium oxide to that of the isostructural uranium nitride is 1.032, and this relationship is applied for UN, α-U_2N_3 and a_o of β-U_2N_3. Therefore, the lattice parameter value for UN_2 is calculated as 5.21 A from that for AmO_2. Fig. 3 shows the lattice parameter data obtained by the present author and by others[2,8,12, 24,26,27,34,35], and also the estimated value for the stoichiometric UN_2.

A solid solution between an Mn_2O_3-type and a CaF_2-type cubic compound is reported to occur in the systems: Pr_2O_3 - PrO_2, Tb_2O_3 - TbO_2 Am_2O_3 - AmO_2 and Cm_2O_3 - CmO_2. Generally, a solid solution occurs between a trivalent-metal oxide Me_2O_3 and a tetravalent-metal oxide $Me'O_2$. Here, Me_2O_3 are Y_2O_3, and the rare earth C-type sesquioxides, and $Me'O_2$ are CeO_2, ZrO_2, HfO_2, ThO_2, NpO_2, UO_2 and PuO_2. For solid solutions in the oxide systems of Pr, Tb, Am and Cm, it is seen that the variation in lattice parameter with O/Me atom ratio is nearly linear, even though intermediate compounds exist. Accordingly, the lattice parameters determined for $UN_{1.75}$ - $UN_{1.80}$ may be connected linearly with the value estimated for UN_2. The relations between the lattice parameter and the N/U ratio in the U_2N_3 - UN_2 system are represented by two straight lines; one is characteristic of U_2N_{3+x} and the other characteristic of UN_{2-y}. Their different slopes and the gap between two lines at $UN_{1.75}$ will suggest that the structure of α-U_2N_3 is not a simple extension of the UN_2 structure.

4.2. Defect Types of α-U_2N_3 and UN_2

Variation in density of U_2N_3 and UN_2 with composition is shown in Fig. 4. Measurements were carried out at 25.0 ± 0.1°C using toluene as a pyknometer fluid. In the single phase region of U_2N_3, the density increases with the N/U atom ratio. For $UN_{1.76}$, observed values are as large as those for $UN_{1.7}$.

In order to examine the nature of nonstoichiometry in α-U_2N_3 and UN_2, the observed changes in density are compared with those calculated for the various possible models. The calculated density will indicate whether the deviation from stoichiometry is due to interstitial atoms or to vacant lattice sites. The theoretical density of a binary stoichiometric compound, MX_s, containing n molecules per unit cell, is given as

$$\rho_s = n(M+sX)/NV \quad (1)$$

where M and X are the atomic weights, s the atom ratio of X-to-M, N Avogadro's number and $V(=a_o^3)$ the volume of the unit cell, and a_o the lattice parameter. For a nonstoichiometric compound, $MX_{s\pm\delta}$, the theoretical densities resulting from the two defect types are calculated from the following equations. The densities in the $MX_{s+\delta}$ region are

$$\rho_{Xi} = n[M+X(s+\delta)]/NV \quad (2)$$

for interstitial X, and

$$\rho_{V_M} = ns[M/(s+\delta)+X]/NV \quad (3)$$

for vacant M, and those in the region of $MX_{s-\delta}$ are

$$\rho_{V_M} = n[M+X(s-\delta)]/NV \quad (4)$$

for vacant X, and

$$\rho_{Mi} = ns[M(s-\delta)+X]/NV \quad (5)$$

for interstitial M.

Substituting the values 238.03, 14.01, 4 and 1.5 for M, X, n and s, respectively, in Eqns (2) and (3), and using half the lattice parameters for the sequinitride given in Fig. 2, the theoretical densities for U_2N_{3+x} can be obtained. With s = 2 and the lattice parameters for the dinitride shown in Fig. 2, the densities for UN_{2-y} can be similarly obtained. The results of calculation for Eqns (2) to (5) are shown by the four solid lines in Fig. 4. As indicated in the figure, if the defect structure of α-U_2N_3 is due to cation vacancies, the density should decrease as the N/U atom ratio increases. The measured densities, however, increase as the N/U ratio increases. Therefore, the fact shows that the deviation from the stoichiometry in the U_2N_3 region is predominantly due to the presence of the interstitial nitrogen atoms rather than to the cation vacancies. In the UN_{2-y} region, it can be easily deduced that the nonstoichiometry is caused by the nitrogen vacancies.

5. Crystal Structure of Nonstoichiometric U_2N_3

The defect type in a nonstoichiometric compound may also be confirmed by determining the crystal structure. Here the effect of nonstoichiometry on the crystal structure of U_2N_3 is examined.

5.1. Structure of α-U_2N_3

α-U_2N_3 crystallizes in the Mn_2O_3-type body-centered cubic structure [26]. The ideal unit cell contains 16 formula units, with two uranium atom positions U(I) and U(II), and one nitrogen atom position N(I). The space group of the nitride is Ia3 with the atoms in the positions[37]:

U(I):8(b) 1/4 1/4 1/4; 1/4 3/4 3/4; 3/4 1/4 3/4; 3/4 3/4 1/4; B.C.
U(II):24(d) $\pm$(u 0 1/4; 1/4 u 0; 0 1/4 u; $\bar{u}$ 1/2 1/4; 1/4 $\bar{u}$ 1/2; 1/2 1/4 $\bar{u}$); B.C.
N(I):48(e) $\pm$(x y z; x $\bar{y}$ 1/2-z; 1/2-x y $\bar{z}$; $\bar{x}$ 1/2-y z; z x y; 1/2-z x $\bar{y}$; z 1/2-x y; z $\bar{x}$ 1/2-y; y z x; $\bar{y}$ 1/2-z x; y $\bar{z}$ 1/2-x; 1/2-y z $\bar{x}$); B.C.

The structure has 16 nitrogen vacancy positions, denoted as N(II):16(c). They become filled with nitrogen atoms, as U_2N_3 with the ideal structure dissolves more nitrogen than represented by its chemical formula.

The positions of U(II) sites have one parameter u. This parameter is examined from X-ray[3,20,26,33] and neutron diffraction[21,33]. According to Rundle et al.[26] and Anselin[3], the parameter changes continuously with increase in nitrogen content to the N/U ratio of 1.75. However, Tobisch and Hase[33] and Masaki et al.[20] indicate that the parameter is a constant value even if nitrogen content is varied. They obtained -0.021 and -0.015, respectively. The parameters for nitrogen atom positions, N(I) and N(II), also have been determined from neutron diffraction for the nitrides with the N/U atom ratio of 1.600, 1.655, 1.685 and 1.740. The parameters in the position 48(e), x, y, z, are 0.38, 0.14, 0.38, respectively, and that in the position 16(c), v, is 0.15[21,33]. From these results, it is concluded that all uranium and nitrogen positions in U_2N_3 are not affected by nitrogen dissolution. In the analysis, no empty site is found at the position N(I):48(e). The excess nitrogen atoms,

causing the deviation from the ideal composition of U_2N_3, are distributed only at N(II):16(c) sites without the structure change. It is shown that the results of the structural analysis are consistent with those of the lattice parameter and density measurements. The crystal structure of U_2N_3 is shown in Fig. 5, as a projection along a cubic axis.

5.2. Structure of the Intermediate Nitride

The X-ray and neutron diffraction pattern of $UN_{1.76}$ are quite different from that of U_2N_3. Although a few very weak reflections in the pattern are still visible, a number of weak reflections, deduced from the Mn_2O_3-type structure, are detected no longer. The X-ray and neutron diffraction patterns for $UN_{1.74}$ and $UN_{1.76}$ are shown in Fig. 6. The figures disclose the difference between two crystal systems of both the nitrides. The profiles for 220, 311, 222, 331, 420 and 422 reflections give twice, or more, the half width of the nitrides with the N/U atom ratio below 1.75. Broadening of the line profiles of $UN_{1.76}$ is possibly explained on the basis of the rhombohedral pseudo-cell, which comes from only a slight distortion of the ideal CaF_2-type cell. The CaF_2-type structure with the lattice parameter of 5.29 A can be transformed into the rhombohedral structure with the lattice parameter of $a_o' = 6.50$ A, $\alpha = 99.7°$, and with the volume of 7.4 times of the CaF_2 unit cell. It is shown that broadening of the line profiles is caused by overlapping of some diffraction lines. Similarly to the case of the systems composed between a sesquioxide and a dioxide in lanthanide and actinide oxides, the rhombohedral modification is also found in the U - N system.

6. Thermodynamic Properties of α-U_2N_3

6.1. Equilibrium Nitrogen Pressure

The decomposition pressure of U_2N_3 have been studied using the direct manometric measurement method in the temperature range between 600 and 1300°C[10,14,18,19,23,31]. The decomposition of U_2N_3 into UN is represented by the following equation:

$$U_2N_{3+x_0} = 2\ UN + (1+x_0)/2\ N_2 \qquad (6)$$

where x_U is the value at the U-rich phase boundary, and $x_0 = 0.08$. Although the $\alpha \rightarrow \beta$ phase transition has been reported to occur at temperatures above 800°C, the formation of β-U_2N_3 is not observed during the pressure measurements. The equilibrium pressures over the two phases of $UN + U_2N_3$ are expressed by

$$\log p_{N_2}(\text{atm}) = 7.201 - 1.174\times10^{-4}/T \qquad (7)$$

Nitrogen dissolution in U_2N_3 of the single phase can be expressed as:

$$U_2N_{3+x} + \delta x/2\ N_2 = U_2N_{3+x+\delta x} \qquad (8)$$

The nitrogen pressure over the single phase is varied as a function of temperature and composition. Measurements are performed by using an apparatus containing a thermobalance and a pressure measurement system[13, 19], or by using the Sievert apparatus[10,23]. The pressure - composition isotherms have been examined at a given temperature between 500 and 1100°C [10,13,19,23]. Fig. 7 shows the results obtained by Fujino and Tagawa[13], which are in good agreement with those by Bugl and Bauer[10]. The data indicate that the dependence of log p on the N/U ratio is linear, and that the slope of these isotherms becomes steeper with decreasing in the temperature from 1000 to 500°C. Although the N-rich phase boundary of U_2N_3 should be at $UN_{1.75}$, it is difficult to obtain the isotherm at the composition beyond the N/U ratio of 1.71, because it requires very long time to attain an equilibrium. Figure 8 shows a plot of log p versus 1/T at given N/U atom ratios between 1.56 and 1.70.

6.2. Thermodynamic Properties of α-U_2N_3

Thermodynamic functions of the decomposition of α-U_2N_3 are obtained using Eqns (6) and (7). The change in Gibbs free energy for $U_2N_{3.08}$ at temperatures between 750 and 1050°C is given as

$$\Delta G^\circ_T = -29{,}000 + 17.80\ T(\text{cal/mol}) \qquad (9)$$

The standard heat and entropy of the decomposition at 298.15K may be derived from Eqn (9), provided that the thermodynamic functions are available for UN(s), N_2(g), and U_2N_3(s). However, no high temperature

heat content or enthalpy increment has determined. The heat content for $U_2N_{3.08}$ was estimated from extrapolation of the low-temperature Cp values:

$$Cp^\circ(U_2N_{3.08}) = 31.690 + 9.220\times10^{-3}T - 8.0296\times10^5/T^2 \text{(cal/deg.mole)}$$

Using the equation, the author[29] obtained the heat of decomposition to be ΔH°_{298}(3rd) = 33.4 kcal/mol.

Partial molar quantities were calculated from the data of Fig. 8 for a given composition. Figure 9 shows the partial molar free energy $\Delta\bar{G}(N_2)$ for the N/U atom ratio of 1.56 to 1.68 in the temperature range from 800 to 1400K. It is seen in the figure that the variation in $\Delta\bar{G}(N_2)$ with N/U ratio is linear at the measured temperature region.

Partial molar entropy and enthalpy are obtained from the intercept and the slope of the straight lines in Fig. 8, respectively. The values of $\Delta\bar{S}(N_2)$ are shown in Fig. 10. As the nitrogen content of the nitride increases, the partial molar entropy increases from -32.2 at $UN_{1.56}$ to -23.1 cal/deg.mol N_2 at $UN_{1.68}$. The partial molar enthalpy $\Delta\bar{H}(N_2)$, as shown in Fig. 11, also increases from -51.0 at $UN_{1.56}$ to -24.3 kcal/mol N_2 at $UN_{1.68}$. No maximum and minimum are found in the curve of $\Delta\bar{S}(N_2)$ versus N/U ratio, and also in the curve of $\Delta\bar{H}(N_2)$ versus N/U ratio. Therefore, it may be concluded that nitrogen is dissolved in the single phase of U_2N_3 without any change of the structure. The results are consistent with those obtained from the lattice parameter and density measurements, and from the structure analysis.

For the systems Ce_2O_3 - CeO_2[9], Pr_2O_3 - PrO_2[17], Pu_2O_3 - PuO_2[25], and Am_2O_3 - AmO_2[11], thermodynamic functions have been measured in the wide nonstoichiometric range of composition. Every oxide system has the continuous solid solution between the sesquioxide and the dioxide, as already mentioned. Figure 12 shows the partial molar entropies of these oxide systems together with the results measured on U_2N_3. The variation in the partial molar entropy with the O/Me ratio is nearly linear in the systems of Pu - O and Am - O. The slope of $\Delta\bar{S}(O_2)$ versus O/Me ratio for the Pr - O system is similar to that of $\Delta\bar{S}(N_2)$ versus N/U ratio of the present work. On the contrary, $\Delta\bar{S}(O_2)$ for the systems Ce - O, Pu - O and Am - O decrease with increasing of the O/Me ratio. Generally, the predominant feature of the correlation of partial molar entropy with

composition is a decrease in $\Delta\overline{S}(O_2)$ with increasing oxygen content in the nonstoichiometric region, and this is also found in other compounds. The trend is attributed to the domination of partial molar entropy value in the configuration term, whatever the model of defect structure is taken. In fact, the results, calculated on the nonstoichiometric U_2N_3 using a statistical model[13], show that the theoretical $\Delta\overline{S}(N_2)$ value decreases with increasing in the N/U ratio. However, the experimental $\Delta\overline{S}(N_2)$ value increases with the N/U ratio. It is not yet clear what is the reason of the discrepancy between the theoretical and the experimental $\Delta\overline{S}(N_2)$. It might be thought that the excess nitrogen is dissolved in U_2N_3 to form the ordered state.

This paper was presented at the Japan - US Joint Seminar on "Defects and Diffusion in Solids" held at Tokyo, October 4 - 6, 1976.

References

[1] Y. Akimoto, J. Inorg. Nucl. Chem., 29 (1967) 2650.
[2] F. Anselin, J. Nucl Mater., 10 (1963) 301.
[3] F. Anselin, Fontenay-auxRoses (France) Rapport CEA-R 2988 (1966).
[4] L. B. Asprey, F. H. Ellinger, S. Fried and W. H. Zachariasen, J. Am. Chem. Soc., 77 (1955) 1708.
[5] R. Benz and M. G. Bowman, J. Am. Chem. Soc., 88 (1966) 264.
[6] R. Benz, G. Balog and B. H. Baca, High Temp Sci., 2 (1970) 221.
[7] R. Benz and W. B. Hutchinson, J. Nucl. Mater., 36 (1970) 135.
[8] H. J. Berthold und C. Delliehausen, angew. Chem., 78 (1966) 750.
[9] D. J. M. Bevan and J. Kordis, J. Inorg. Nucl. Chem., 26 (1964) 1509.
[10] J. Bugl and A. A. Bauer, Compounds of Interest in Nuclear Reactor Technology, ed. by J. T. Waber, P. Chiotti and W. N. Miner (Edwards Bros. Inc., Ann Arbor, Mich., 1964) 215.
[11] T. D. Chikalla and L. Eyring, J. Inorg. Nucl. Chem., 29 (1967) 2281.
[12] J. F. Counsell, R. M. Dell and J. F. Martin, Trans. Faraday Soc., 62 (1966) 1736.
[13] T. Fujino and H. Tagawa, J. Phys. Chem. Solids, 34 (1973) 1611.
[14] P. Gross, C. Hayman and H. Clayton, Thermodynamics of Nuclear Materials (IAEA, Vienna, 1962) 653.
[15] C. L. Hoenig, J. Am. Ceram. Soc., 54 (1971) 391.
[16] H. Holleck and T. Ishii, Thermal Analysis 1971, Vol. 2 (Birkhäuser Verlag, Basel, 1972) 137.
[17] M. S. Jenkins, R. P. Turcotte and L. Eyring, The Chemistry of Extended Defects, ed. by L. Eyring and M. O'Keeffe (North-Holland, Amsterdam, 1970) 36.
[18] M. Katsura and T. Sano, J. Nucl. Sci. Tech., 4 (1967) 283.
[19] P. E. Lapart and R. B. Holden, in ref. [10], p.225.
[20] N. Masaki, H. Tagawa and T. Tsuji, J. Nucl. Mater., 45 (1972/1973) 230.
[21] N. Masaki and H. Tagawa, J. Nucl. Mater., 57 (1975) 187.
[22] N. Masaki and H. Tagawa, J. Nucl. Mater., 58 (1975) 241.
[23] F. Müller and H. Ragoss, Thermodynamics of Nuclear Materials (IAEA, Vienna, 1968) 257.
[24] A. Naoumidis, Kernforschungsanlage Jülich (Germany) Jül-472-RW (1967).
[25] M. H. Rand, Atomic Energy Rev., Vol. 4, Special Issure No. 1 (IAEA, Vienna, 1966) 225.

[26] R. E. Rundle, N. C. Baenzieger, A. S. Wilson and R. A. McDonald, J. Am. Chem. Soc., 70 (1948) 99.

[27] Y. Sasa and T. Atoda, J. Am. Ceram. Soc., 53 (1970) 102.

[28] H. J. Stöcker und A. Naoumidis, Ber. Deutsch. Keram. Ges., 43 (1966) 724.

[29] H. Tagawa, J. Nucl. Mater., 41 (1971) 313.

[30] H. Tagawa and N. Masaki, J. Inorg. Nucl. Chem., 36 (1974) 1099.

[31] H. Tagawa, J. Nucl. Mater., 51 (1974) 78.

[32] D. H. Templeton and C. H. Dauben, J. Am. Chem. Soc., 75 (1953) 4560.

[33] J. Tobisch and W. Hase, Phys. Stat. Sol., 21 (1967) K11.

[34] R. Troc, J. Solid State Chem., 13 (1975) 14.

[35] W. Trezbiatowski and R. Troc, Bull. L'Acad. Polo. Sci. Ser. Sci. Chim., 12 (1964) 681.

[36] D. A. Vaughan, J. Metals, 8 (1956) 78.

[37] R. W. G. Wyckoff, Crystal Structures, 2nd ed., Vol. 2 (Intersci. Pub., 1964) 1.

Table I. Periodic classification of nitrogen compounds.

	IA	IIA	IIIA	IVA	VA	VIA	VIIA	VII			IB	IIB	IIIB	IVB	VB	VIB	VIIB	O
1	H_3N																	
2	Li_3N	Be_3N_2											BN	$(CN)_M$		N_2O NO NO_2		
3	Na_3N	Mg_3N_2											AlN	Si_3N_4	P_3N_5	S_4N_4		
4		Ca_3N_2	ScN	$\overline{Ti_2N}$ $\overline{TiN}$	$\overline{V_2N}$ $\overline{VN}$	$\overline{Cr_2N}$ $\overline{CrN}$	$\overline{Mn_4N}$ $\overline{Mn_2N}$ $\overline{Mn_3N_2}$	$\overline{Fe_4N}$ $\overline{Fe_2N}$	Co_4N Co_3N Co_2N	Ni_4N Ni_3N	Cu_3N	Zn_3N_2	GaN	Ge_3N_4	AsN	$(SeN)_n$		
5		Sr_3N_2	YN	$\overline{ZrN}$	$\overline{Nb_2N}$ $\overline{NbN}$	$\overline{Mo_2N}$ $\overline{MoN}$	TcN				Ag_3N	Cd_3N_2	InN					
6		Ba_3N_2	LnN	$\overline{HfN}$	$\overline{Ta_2N}$ $\overline{TaN}$	$\overline{W_2N}$ $\overline{WN}$						Hg_3N_2	TlN					
7			AnN															

LnN	LaN	CeN	PrN	NdN	PmN	SmN	EuN	GdN	TbN	DyN	HoN	ErN	TmN	YbN	LuN

AnN		$\overline{ThN}$ $\overline{Th_3N_4}$	PaN	UN U_2N_3 UN_2	NpN	PuN	AmN	CmN							

Table II Comparison of lattice parameters between uranium nitrides and americium oxides.

Structure	Uranium nitride (A)		Americium oxide (A)		a_o(Am-O)/a_o(U-N) or c_o(Am-O)/c_o(U-N)
NaCl-type f.c.c.	UN	4.8895	AmO	5.045[1]	1.032
Mn_2O_3-type b.c.c.	α-U_2N_3	10.684	α-Am_2O_3	11.03[32]	1.032
La_2O_3-type h.c.p.	β-U_2N_3	a_o = 3.6983	β-Am_2O_3	a_o = 3.817[32]	1.032
		c_o = 5.831		c_o = 5.971	1.024
CaF_2-type f.c.c.	UN_2*	5.210	AmO_2	5.376[4]	

*The lattice parameter for UN_2 is the estimated value.

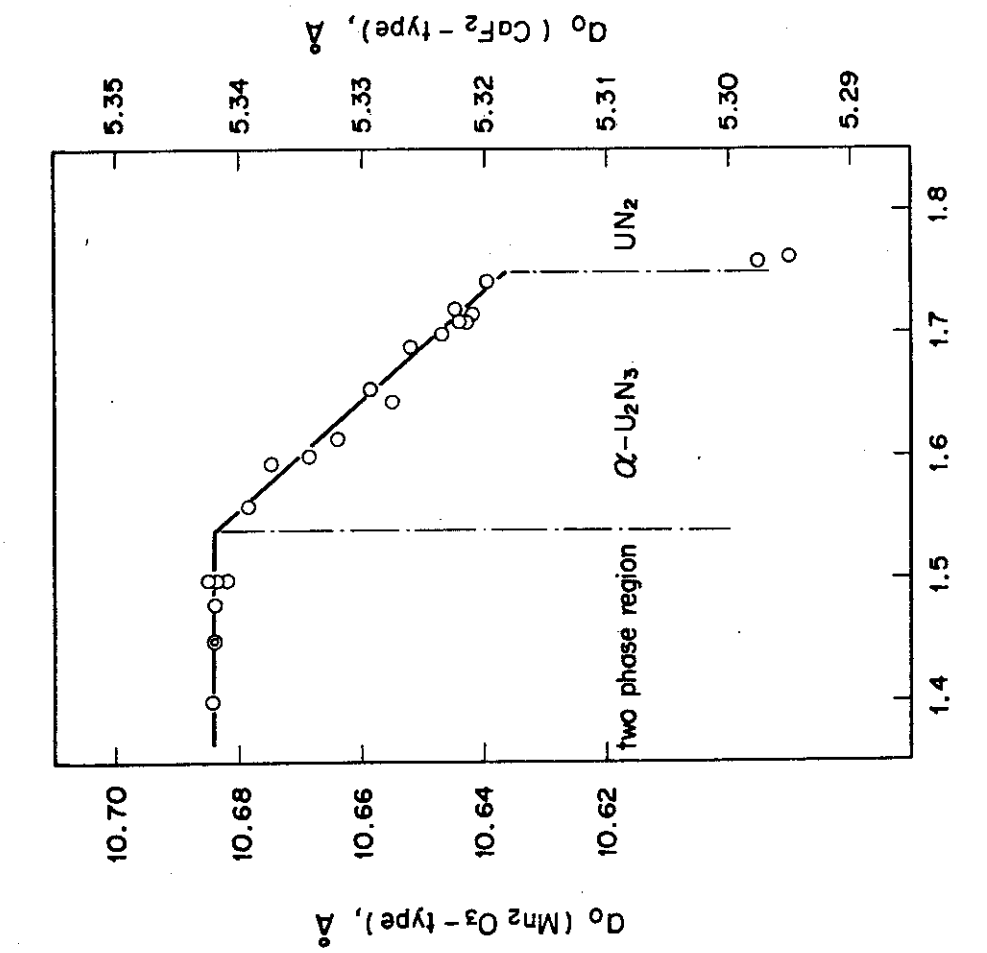

Fig. 2. Variation in lattice parameters of α-U_2N_3 and UN_2 with N/U atom ratio.

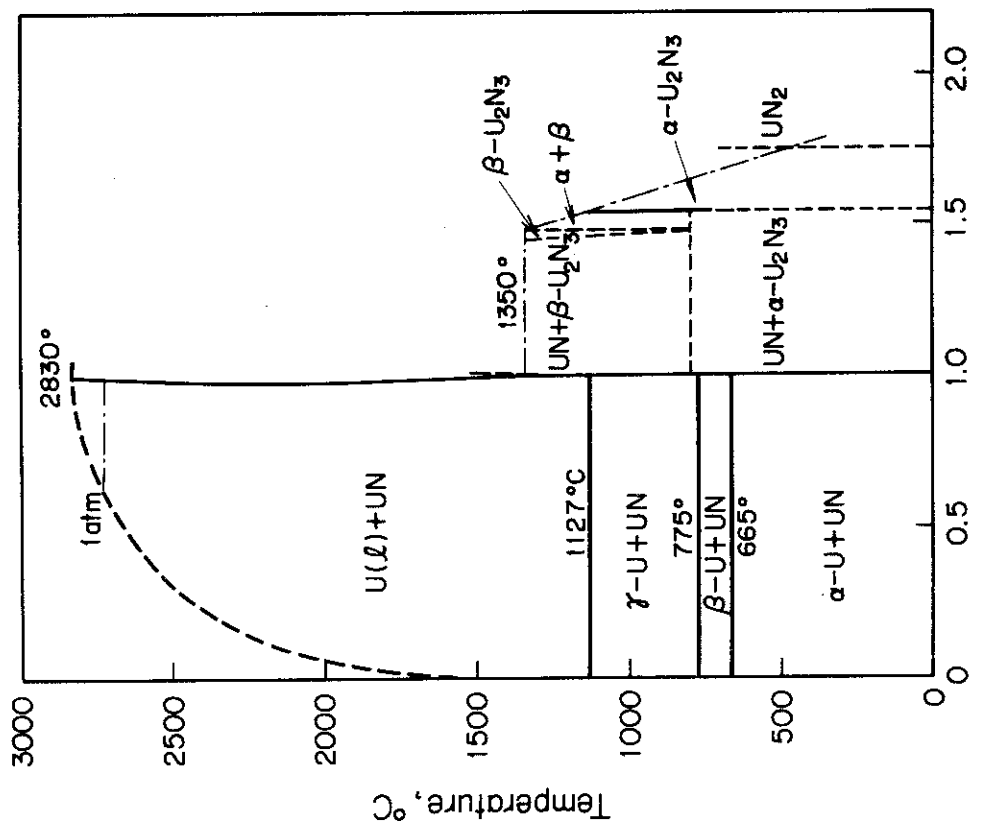

Fig. 1. Phase diagram of the U - N system.

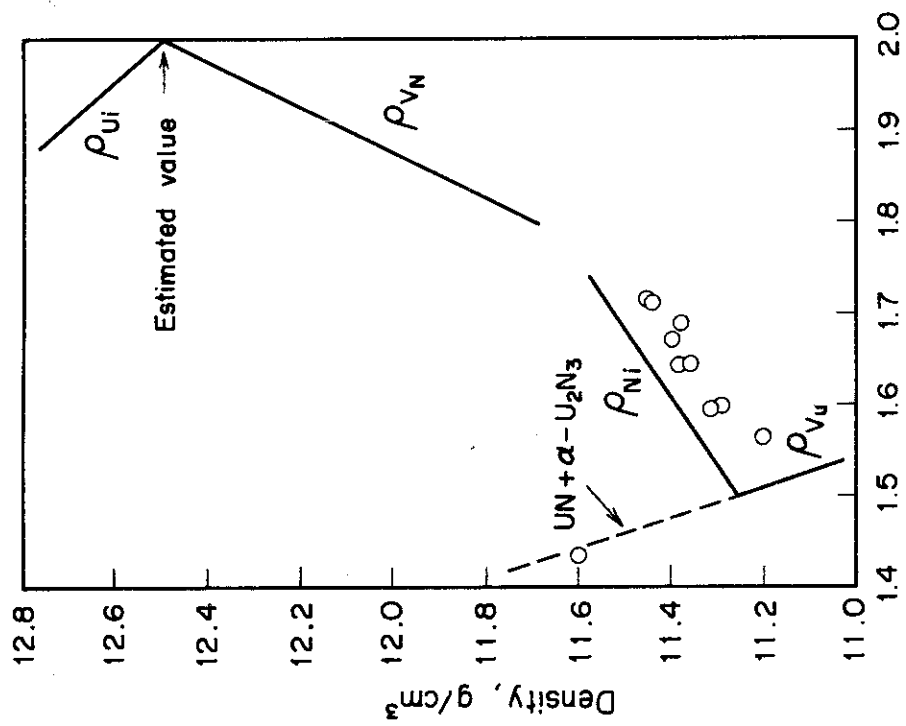

Fig. 4. Density change in the U_2N_3 -UN_2 system.

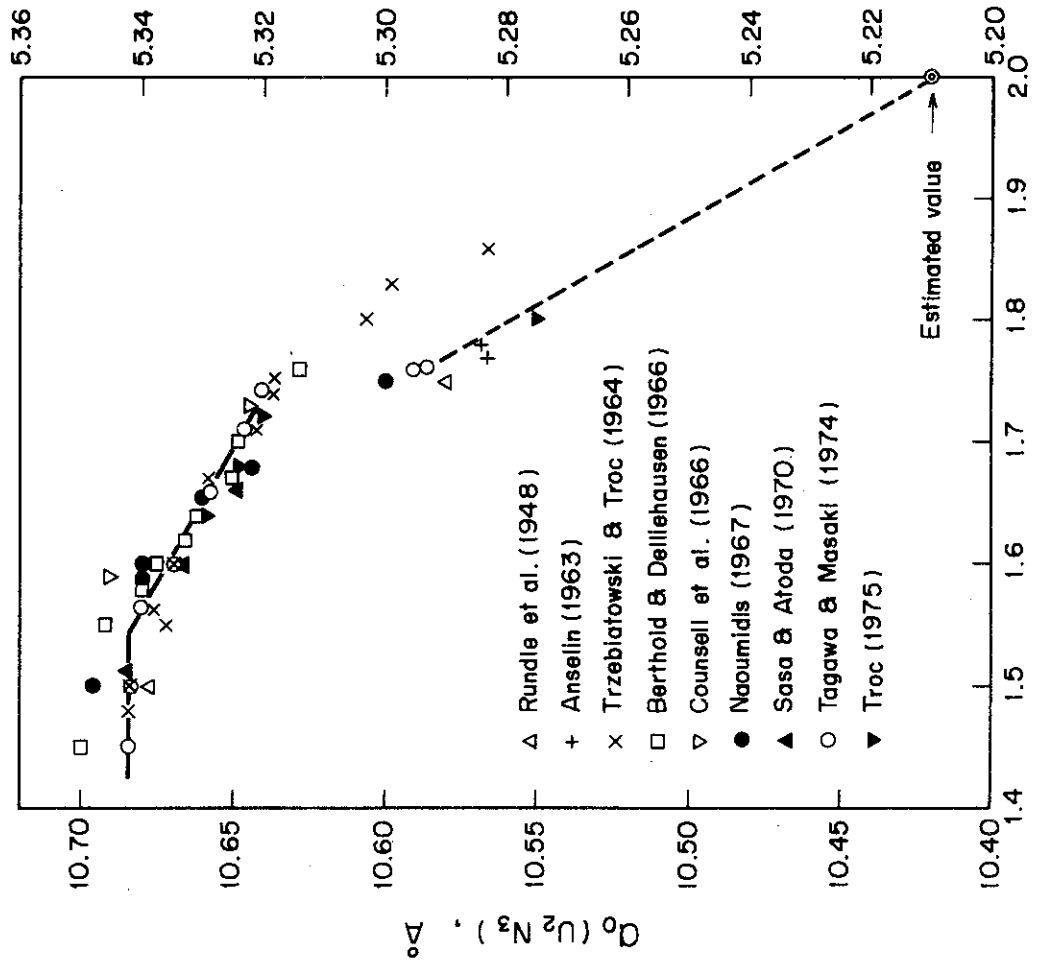

Fig. 3. Lattice parameter change in the U_2N_3 - UN_2 system.

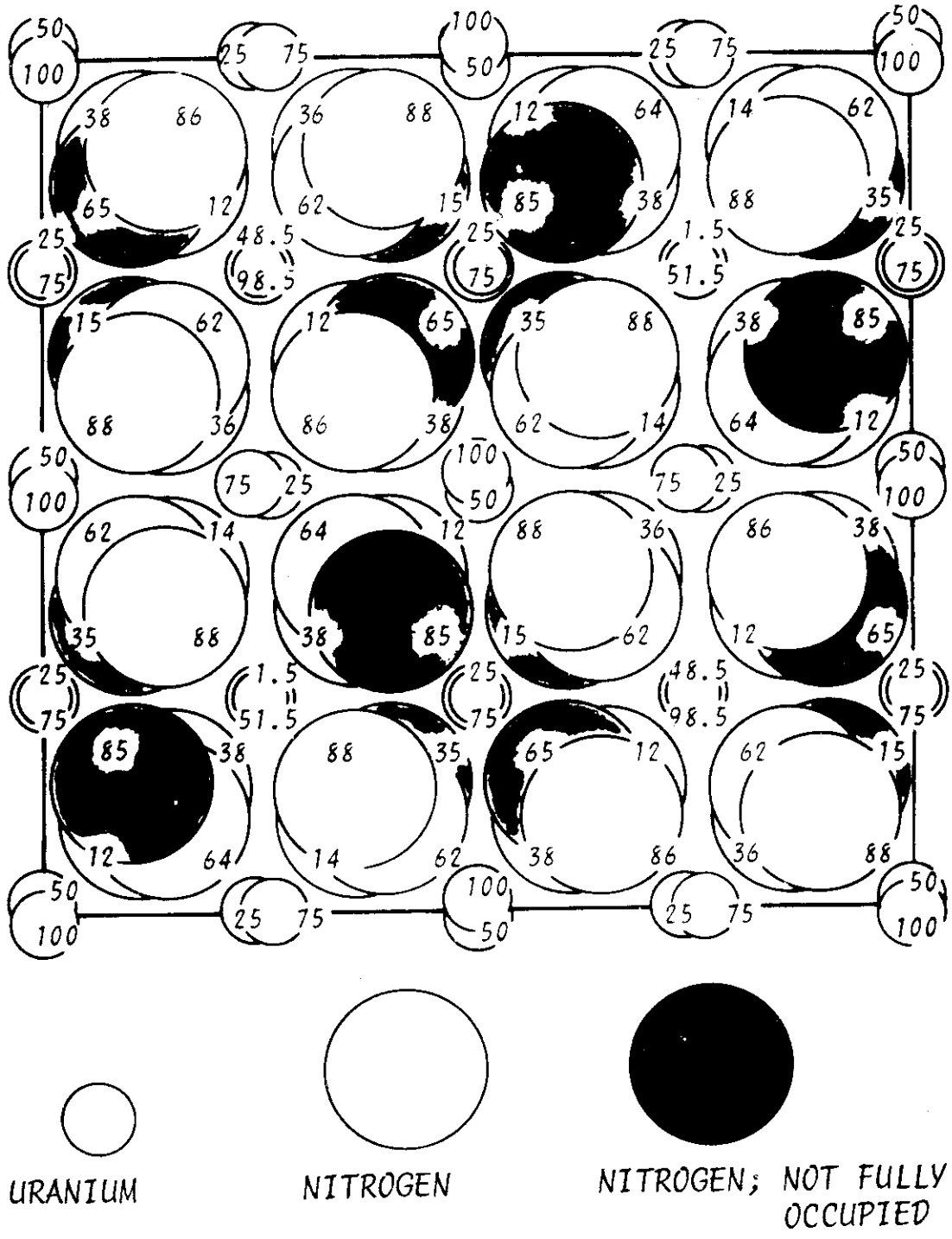

Fig. 5. Crystal structure of nonstoichiometric U_2N_3 projected on (001).

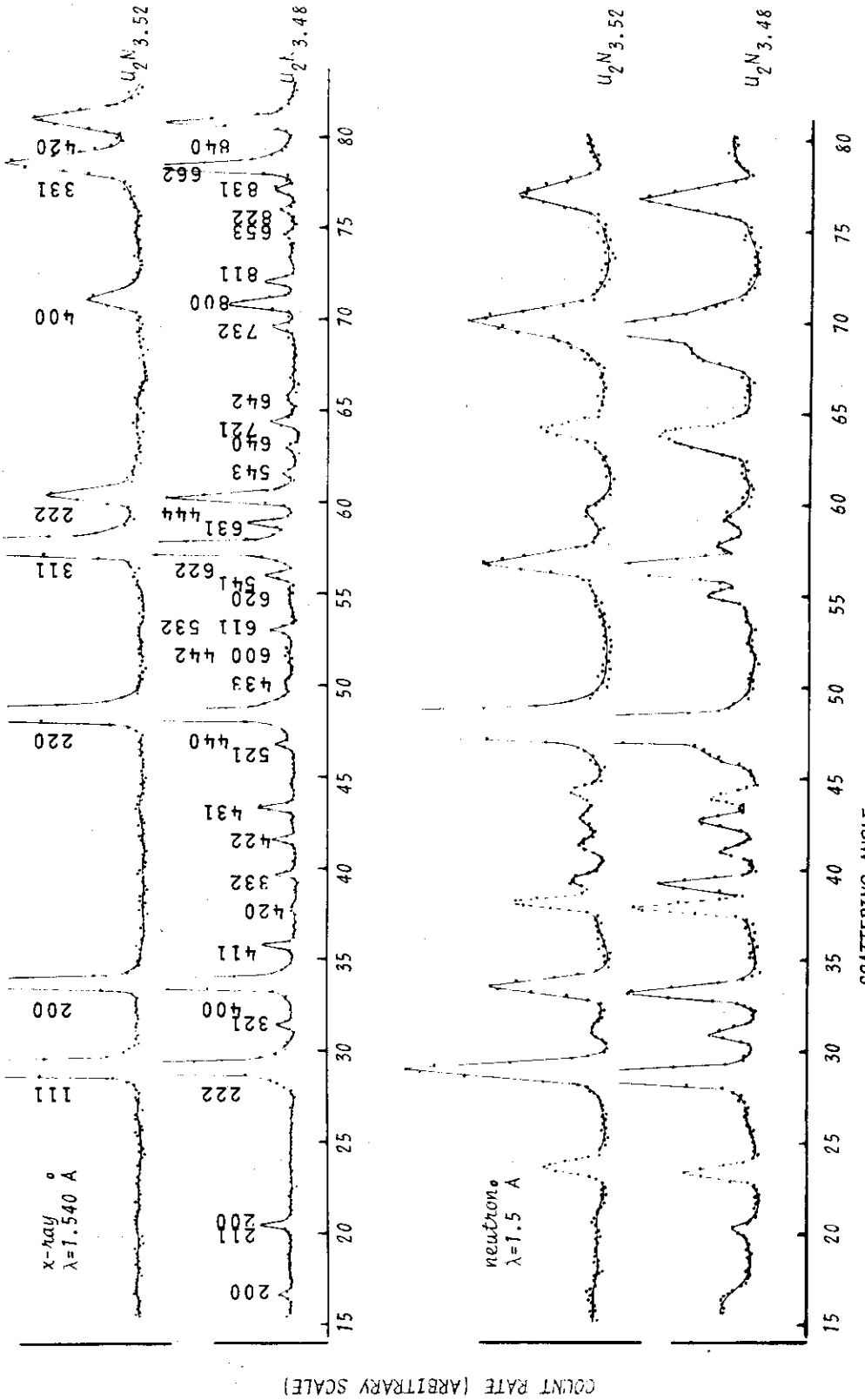

Fig. 6. X-ray and neutron diffraction patterns of $U_2N_{3.48}$ and $U_2N_{3.52}$.

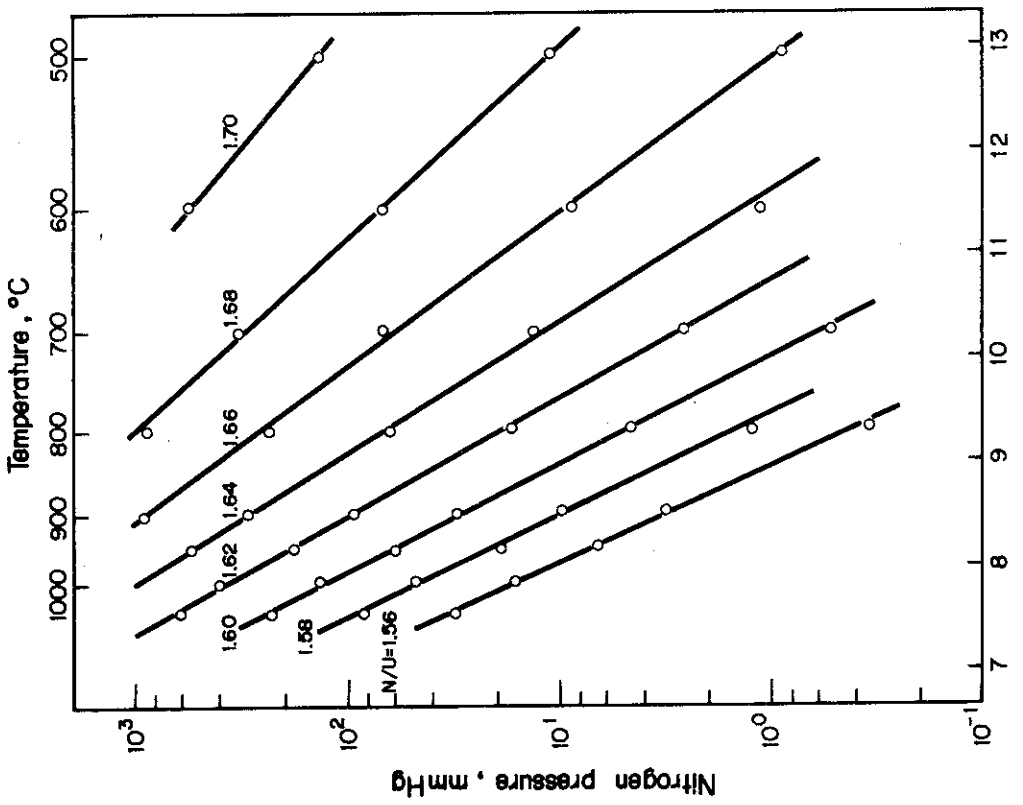

Fig. 8. Nitrogen pressures vs. 1/T for various N/U ratios in the U_2N_3 single phase region.

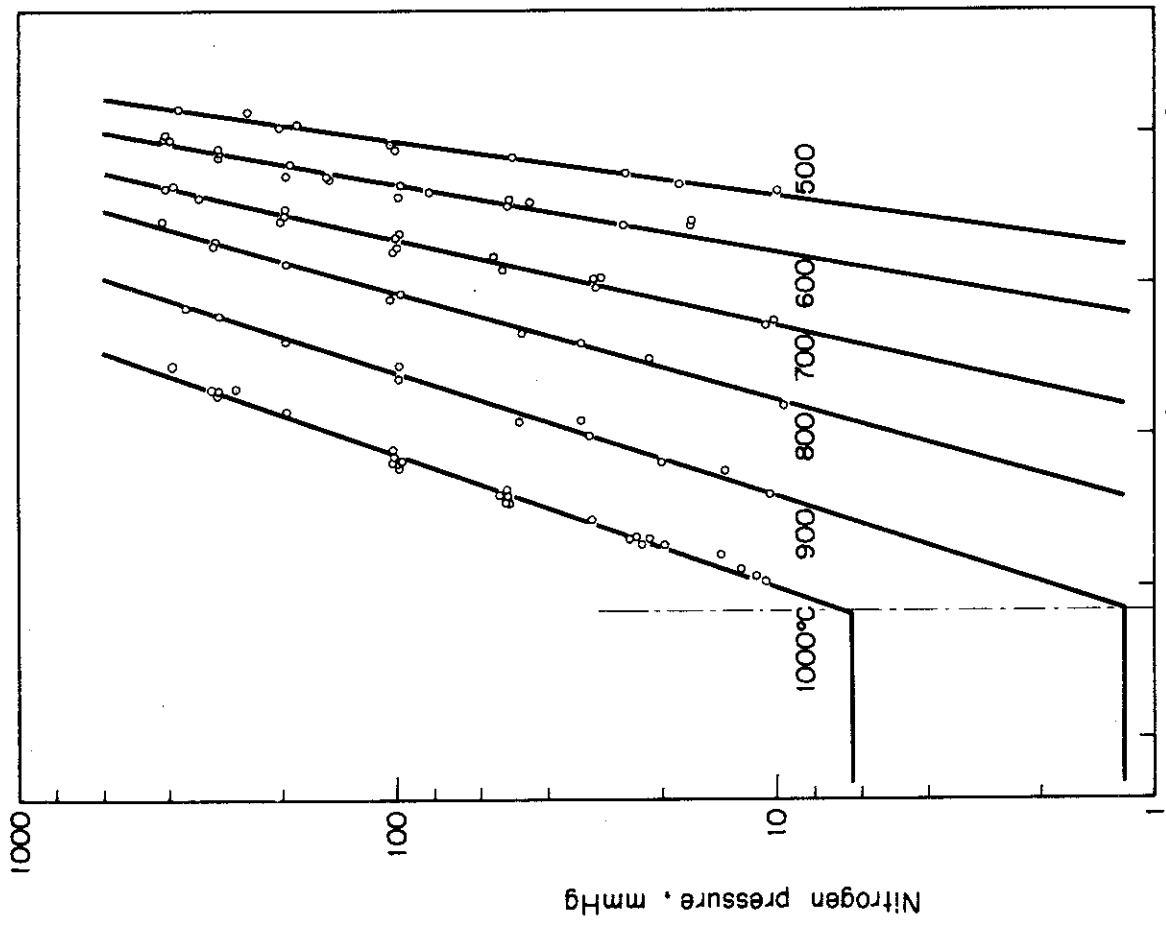

Fig. 7. Pressure - composition isotherms in the U_2N_3 single phase region at temperatures between 500 and 1000°C.

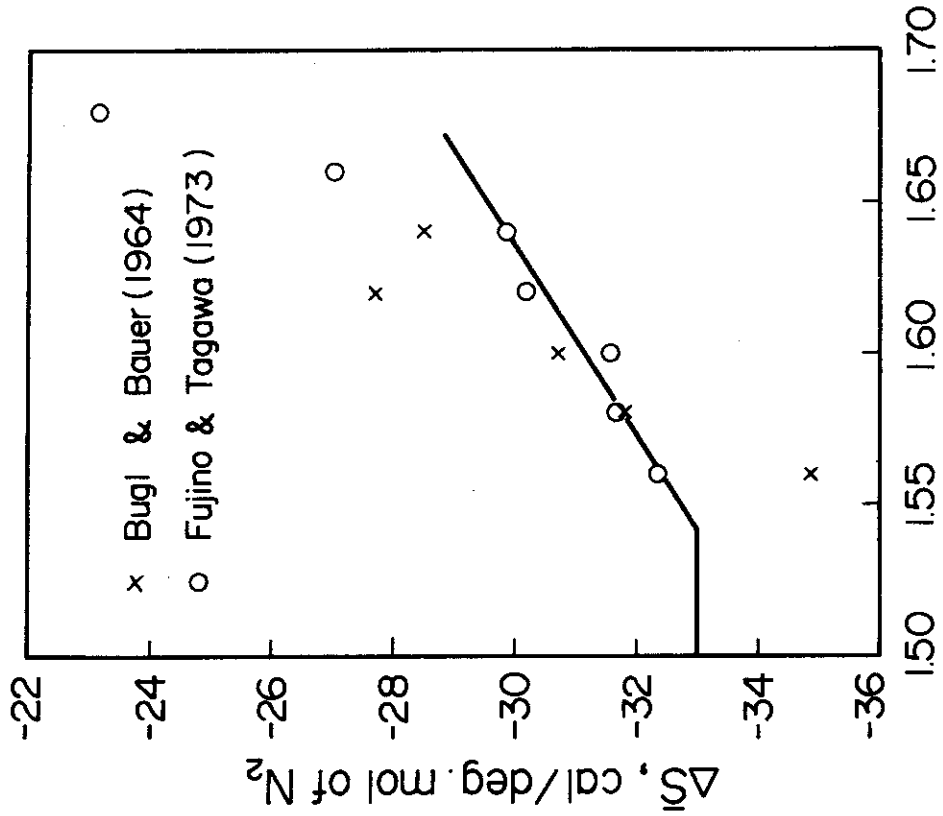

Fig. 10. Variation in partial molar entropy with N/U atom ratio.

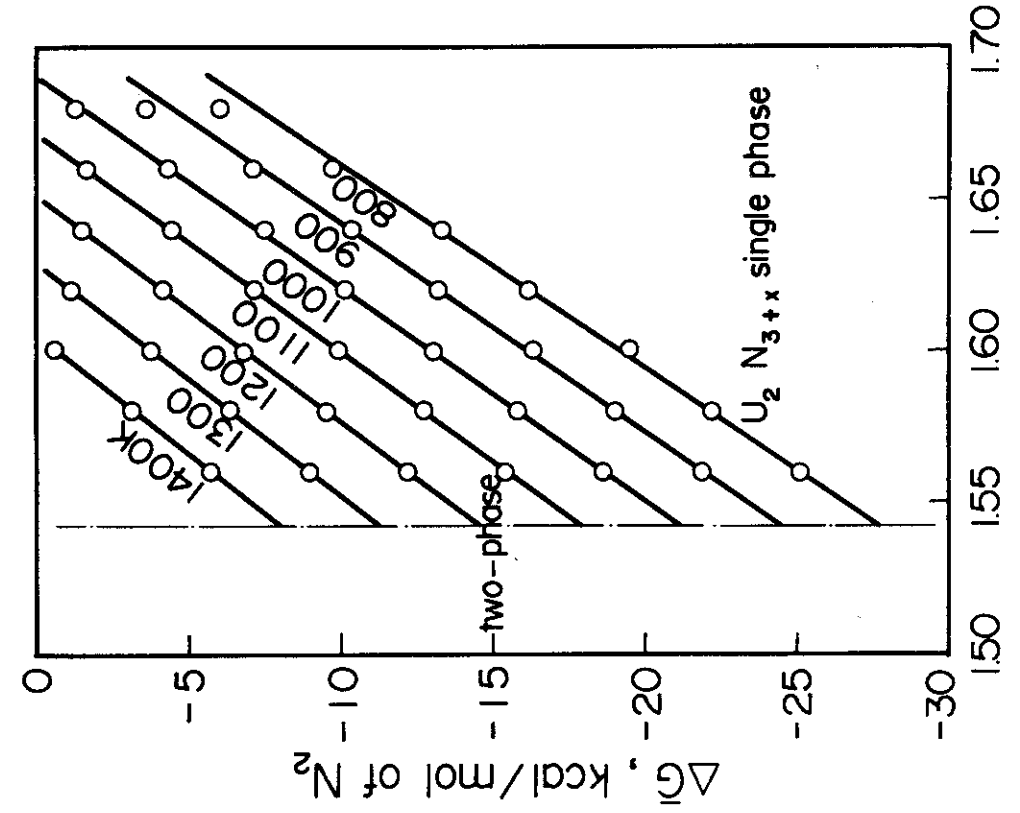

Fig. 9. Variation in partial molar free energy with N/U atom ratio.

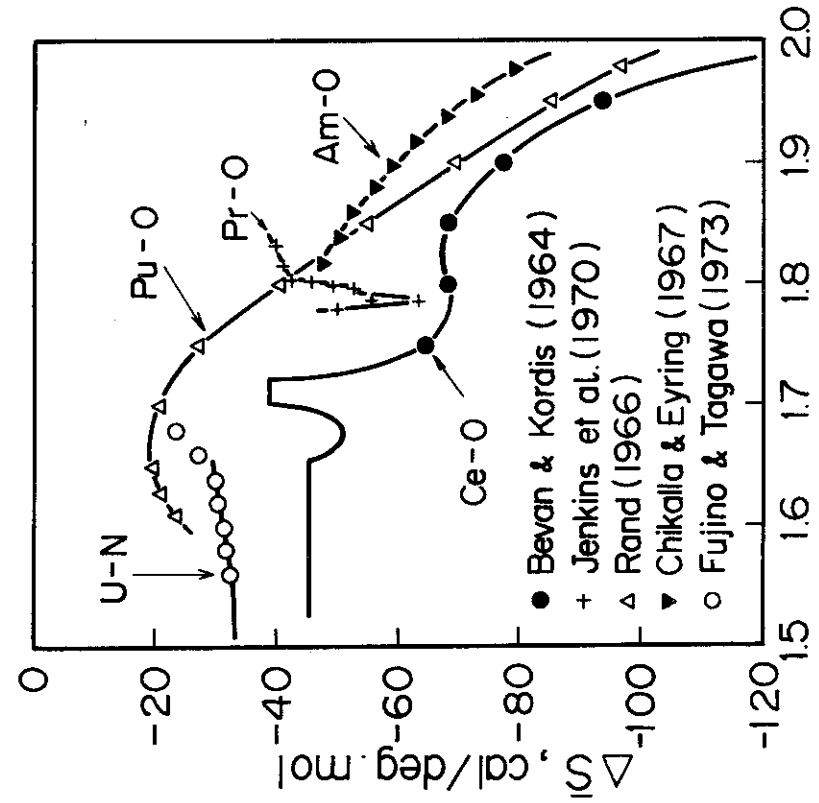

Fig. 12. Variation in partial molar entropies of the systems, Ce-O, Pr-O, Pu-O, Am-O and U-N as a function of composition.

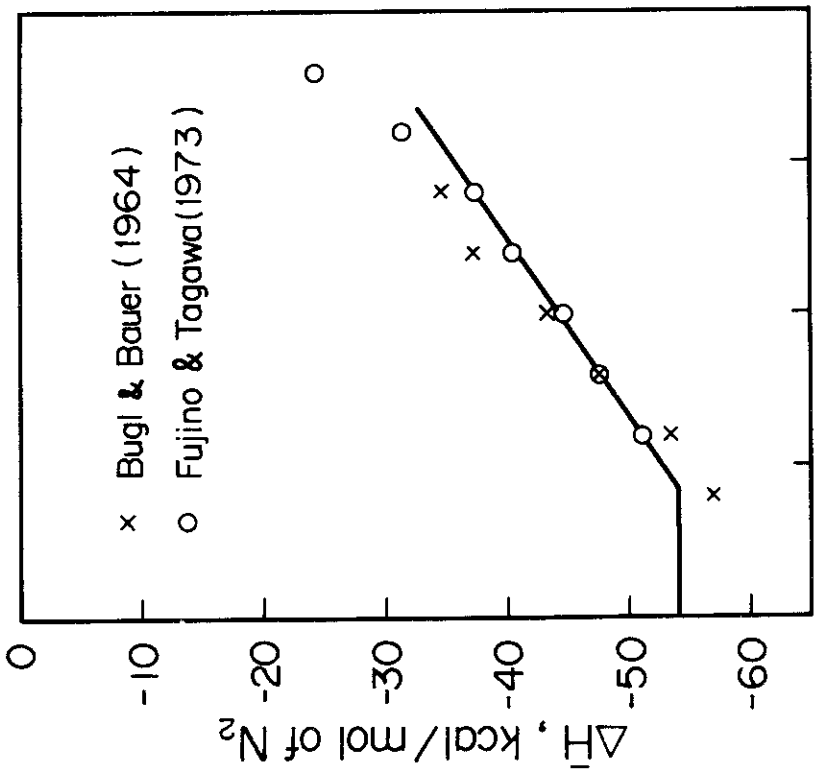

Fig. 11. Variation in partial molar enthalpy with N/U atom ratio.